1 October 1999

ELSEVIER

Optics Communications 169 (1999) 75–80

OPTICS COMMUNICATIONS

www.elsevier.com/locate/optcom

Experimental investigation of wavelength-tunable WADM and OXC devices using strain-tunable fiber Bragg gratings

Shien-Kuei Liaw [a,d,*], Keang-Po Ho [b], Chinlon Lin [c], Sien Chi [a]

[a] *Institute of Electro-Optical Engineering, National Chiao-Tung University, PO Box 75, Yang-Mei 326, Hsin-chu, Taiwan*
[b] *Department of Information Engineering, The Chinese University of Hong Kong, Shatin, New Territories, Hong Kong*
[c] *Tyco Submarine Systems Labs, Eatontown, NJ 07724, USA*
[d] *Department of Electrical Engineering, Da-Yeh University, Chang-Hua, Taiwan*

Received 29 January 1999; received in revised form 20 July 1999; accepted 21 July 1999

Abstract

Two reconfigurable wavelength add/drop multiplexer (WADM) and optical cross-connect (OXC) devices based on strain-tunable fiber Bragg gratings (ST-FBGs) are proposed. The feasibility of WADM is verified by measuring the bit-error-rate performance of the dropped (cross-connect) and pass-through (no cross-connect) channels over a 50- and 100-km standard single-mode fiber for a 2.5 Gb/s system. Compared to back-to-back transmission, a negligible power penalty of only 0.2 dB is observed. © 1999 Published by Elsevier Science B.V. All rights reserved.

Keywords: Wavelength division multiplexing; Wavelength add/drop multiplexer; Optical cross-connect; Fiber Bragg grating; Optical network

1. Introduction

Wavelength add/drop multiplexer (WADM) and optical cross-connect (OXC) switches are essential components in the future dense wavelength division multiplexing (WDM) optical networks, especially in a reconfigurable network topology [1]. Many significant efforts have been devoted to the design of high-capacity, flexible, reliable and transparent multiwavelength optical networks [1,2]. The WADMs allow the network nodes to access a subset of wavelengths in the optical networks, reducing the hardware requirements and processing load in intermediate nodes by handling only pass-through traffic. The OXCs are configurable on a link-by-link basis to allow optimization of capacity allocation, management and scalability of network size. Combination of the WADMs and OXC devices can provide the flexibility to satisfy the reconfigurable requirements and enhance network survivability [3]. Conventional WADMs and OXC devices may use the $1 \times N$ demultiplexer (DMUX) and $N \times 1$ multiplexer (MUX) pair to separate and combine WDM channels. The ability for reconfiguration is introduced by adding space division switches between the DMUX/MUX pair. However, additional optical components for space division switches technologies, such as waveguide directional couplers [4], semiconductor optical amplifiers (SOAs) [5], low-gain erbium-doped fiber

* Corresponding author. Tel.: +886-3481-1845; fax: +886-3481-2175; e-mail: u8424802@cc.nctu.edu.tw

0030-4018/99/$ - see front matter
PII: S0030-4018(99)00403-4

amplifiers (EDFAs) [6] and some other components, are required. The drawbacks of complicated designs, controls, expensive cost and increased insertion losses of these elements have to be solved for vast applications of WADMs or OXCs.

Using arrayed-waveguide gratings (AWGs) and double-gate switches as the key components of WADMs, the merits of these wavelength add/drop filters have been addressed by previous works [7]. On the other hand, fiber-Bragg-grating (FBG)-based WADM/OXC architecture with the features of loss uniformity, higher contrast ratio and low cost is an alternative candidate when design these devices. For the commercial AWG-based OXC device, the adjacent channel crosstalk is typically one order higher than that of FBG-based OXC device for a 200-GHz channel-spacing WDM system. The larger crosstalk will degrade the system performance and restrict the applications of AWG in dense WDM system for wavelength add/drop and/or cross-connect. Also, the insertion loss is high unless SOAs are used for loss compensation. On the other hand, FBG-based WADMs and/or OXC devices have shown many promising characteristics. Several approaches have been proposed or experimentally demonstrated, such as those based on fiber and array waveguide gratings [8], integration of the WADM [9] and OXC device [10] by using reflective FBGs, optical circulators (OCs) and/or optical switches (OSWs). Another proposal is demonstrated by using demultiplexer and tuning property of FBGs to design the OXC device [11]. In this paper, we propose the WADM and the closely related 2×2 OXC device for simultaneously multiple-wavelength add/drop and cross-connect based on strain-tunable FBGs (ST-FBGs) and three-port OCs. An experiment for the WADM device is investigated to verify the WADM device in a 2.5 Gb/s system over 100 km of conventional single-mode fiber.

2. Configuration of WADM and OXC devices

The proposed WADMs as well as OXC devices are composed of a set of ST-FBG chain and two three-port OCs. The number of necessary fiber components is reduced tremendously compared to previous works. For an eight-channel two-fiber system, the total required FBGs and OCs are 32 ($= 4 \times 4 \times 2$) and 8 ($= 4 \times 2$) in Ref. [11], 256 ($= 2^8$) and 2 ($= 2^1$) for the 'parallel' P type building block in Ref. [10], but only 8 and 2 in our proposal, respectively. The 'series' S-type building block in Ref. [10] has the problem that any status change (bar or cross-state) of mechanical optical switches for some channels may interrupt the information transmission of the other $N-1$ channels. Also, the difference in optical attenuation between the higher loss paths and lower loss paths may induce non-uniform loss among channels, and affect the receiver sensitivity and system signal-to-noise ratio (SNR). Using FBGs for wavelength add/drop and cross-connect, central wavelength-shift control of FBG can be achieved by varying the environmental temperature or applying mechanical strain. However, the response speed for temperature variation is slow mainly due to low temperature coefficient (~ 0.015 nm/°C) of FBG. Applying strain, the tuning range of FBG by tensile stress and compressive stress can be up to 10 nm and 32 nm, respectively [12]. Applying strain will change the grating pitch and fiber index. The tuning range as mentioned above is large enough for WDM system with 200 GHz (1.6 nm) channel spacing.

The operating mechanism of a ST-FBG is depicted in Fig. 1(a) and the possible three-port ele-

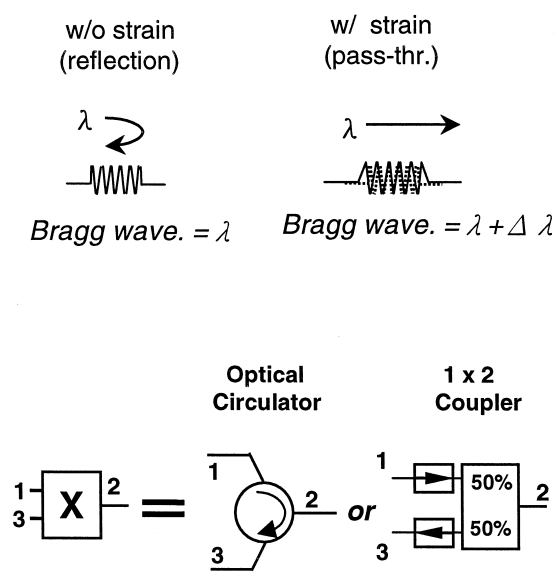

Fig. 1. (a) Operating mechanism of the strain-tunable fiber Bragg gratings; and (b) two possible candidates of the three-port element.

ments are shown schematically in Fig. 1(b). The three-port element could be a three-port OC or a 1×2 50:50 coupler combining two optical isolators to reduce the cost. Fig. 2(a) shows the schematic diagram of two identical WADMs carrying the counter-propagating signals from the opposite directions. The Bragg wavelength of ST-FBG$_i$ is designed to match the WDM-channel signals of λ_i and λ'_i $(1 \le i \le N)$. Before applying strain to the ST-FBG$_i$, the channel signal at λ_i (λ'_i) is reflected and then drops from the same three-port elements containing the I1 (I2) port for the upper (lower) WADM device. At the same time, a set of new WDM channel signals λ'_1, $\lambda'_2 \ldots$ and λ'_N $(\lambda_1, \lambda_2 \ldots$ and $\lambda_N)$ is added into the upper (lower) WADM device via port 1 of the same three-port elements containing the O1 (O2) port, where λ_i and λ'_i $(1 \le i \le N)$ have the same wavelength. On the other hand, if the Bragg wavelength of the ST-FBG$_i$ is shifted about 0.60 nm (in our example) away from its initial position by applying strain, λ_i (λ'_i) may pass-through the WADM and continue its forward propagation. The criterion of wavelength-shift value depends on stopband bandwidth of the ST-FBG and the channel spacing of the WDM system. Because the proposed WADM structure is serial-based operation, the possible effect of wavelength-dependent time delay or dispersion of the FBG should be considered. Usually, FBG only induces dispersion to adjacent channels but not channels far away [13]. Strain tuning of FBG is faster than temperature tuning of FBG. Piezoelectric ceramic transducer (PZT) or acousto-optic tunable fil-

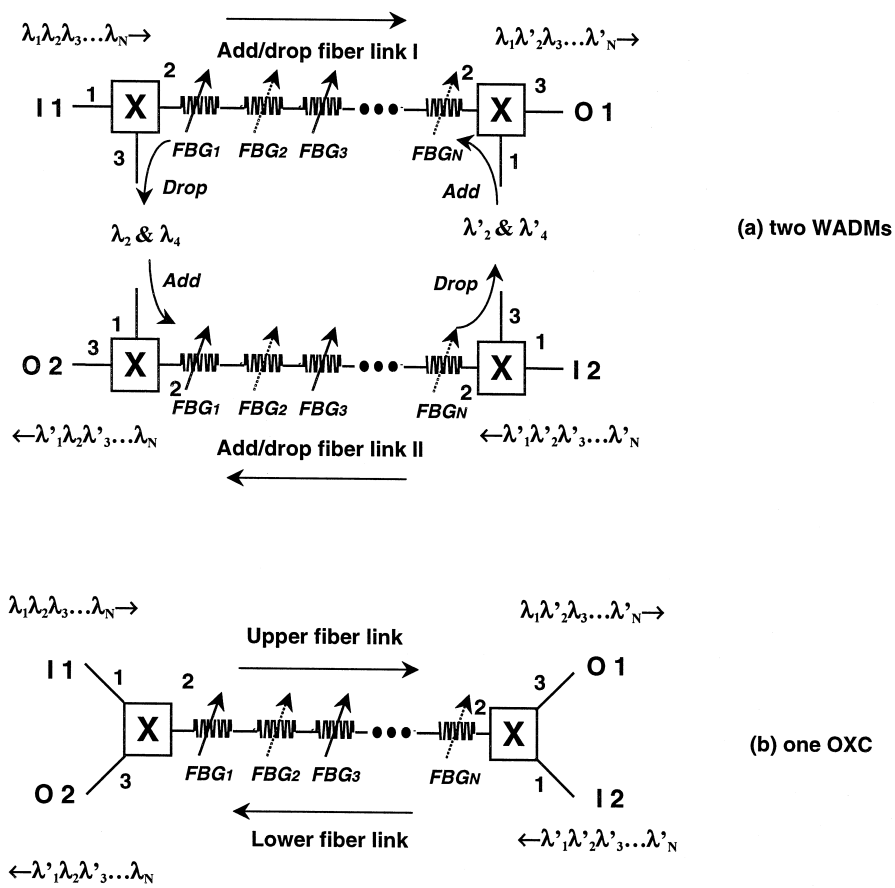

Fig. 2. (a) Two wavelength-add/drop multiplexers; and (b) one reflection type optical cross-connect device. Both the WADM and OXC devices consist of two three-port elements and several strain-tunable fiber-Bragg-gratings.

ter (AOTF) may be used for strain/compress tuning of the FBGs with a fast response speed. For example, when FBG is adhered on a PZT rod and several volts are applied to the PZT, the central wavelength of the FBG can easily be shifted about 1 nm away from its original central wavelength. If a commercialized PZT with 10 KHz response speed is used, the reconfiguration time is sufficiently short for most optical switching networks. To fulfill the requirement in even more high-speed optical switching networks, AOTF with switching speed in the sub-microseconds regime, demonstrated by Riza and Chen [14], is the promising candidate to realize high-speed add/drop function. Temperature control and linear feedback circuit are required to reduce the wavelength fluctuation due to FBGs induce amplitude modulation.

It is interesting to mention that when two WADM devices are connected back to back in a system having two fiber links, a reflection-type 2×2 OXC switch is realized. The dropped channels from fiber link 1 may travel into added port of the fiber link 2, while the dropped channels from fiber link 2 may travel into to added port of the fiber link 1, respectively. The reflection-type OXC device means that any pair of WDM channel signals (λ_i and λ'_i) can be cross-connect from I1 to O2 and from I2 to O1 simultaneously if they are 'reflected' by the corresponding ST-FBG$_i$. To simplify the configuration, another reflection-type OXC switch is shown schematically in Fig. 2(b). One WADM can be used as an OXC device by appropriately choosing the corresponding I1, I2, O1 and O2 ports. There are two input ports of I1 and I2 as well as two output ports of O1 and O2 in the OXC device. These two input ports can operate in the same direction or opposite direction (i.e., bi-directionally) only by rearranging the 3-port elements. Each FBG$_i$ is designed to match the WDM channel signals of λ_i and λ'_i transmitting in the upper and lower fiber links simultaneously. For example, when all wavelengths requiring interchanging, none of the FBG is applied strain and each FBG reflects the individual channel signal back to port 3 of the same three-port element as its input port. In that case, cross-connection of all channel signals is realized by the ST-FBGs. When only some of the wavelengths are interchanged, for example, the exchange of λ_2 and λ_N with λ'_2 and λ'_N. Most of the FBGs except the FBG$_2$ and FBG$_N$ are applied mechanical strain. The WDM channels of λ_1, λ_3, $\lambda_4 \ldots \lambda_{N-1}$ and λ'_1 λ'_3, $\lambda'_4 \ldots \lambda_{N-1} \ldots$ will pass through the OXC device and continue their forward propagation to O1 and O2, respectively. Meanwhile, both the WDM channels of λ_2 and λ_N, λ'_2 and λ'_N are reflected by the corresponding FBG$_2$ and FBG$_N$ and then switched to port O2 (O1) of the three-port element.

3. Experimental setup

ST-FBG is the same as a regular FBG in structure. On applying mechanical strain, ST-FBG can be tuned to longer or shorter wavelength by stretching or squeezing it. The Bragg wavelength λ_B (in nm) is given by

$$\lambda_B = 2n\Lambda \tag{1}$$

where Λ (in nm) is the grating pitch and n is the effective index of the single-mode fiber. The shift in Bragg wavelength for a longitudinal strain ε at a constant temperature ($\Delta T = 0$) is given by the expression [15]

$$\Delta\lambda_B = \lambda_B(1 - P_e)\varepsilon \tag{2}$$

$$P_e = 1/2\, n^2\{P_{12} - \nu(P_{11} + P_{12})\} \tag{3}$$

where P_e is the photoelastic coefficient and has a numerical value of about 0.22, P_{12} and P_{11} represent the components of strain-optic tensor (Pockel coefficients) and ν is the Poisson ratio. The measured strain response at constant temperature is found to be

$$\Delta\lambda_B/(\lambda_B\Delta\varepsilon) = 0.78 \times 10^{-6}\mu\varepsilon^{-1} \tag{4}$$

where μ is 10^{-6}. Fig. 3 shows the experimental configuration of one-channel WADM to verify the system performance. One narrow linewidth, tunable laser source is tuned to 1552.8 nm and externally modulated by a 2.5 Gb/s non-return-to-zero (NRZ) pseudo-random binary sequence. A polarization controller is used to adjust the polarization-state of the laser source for matching to the $LiNbO_3$ intensity modulator. Two spools of 50-km single-mode fiber, locating before and after the WADM, are used as the transmission link. Two erbium-doped fiber amplifiers (EDFAs) with a saturated output power of

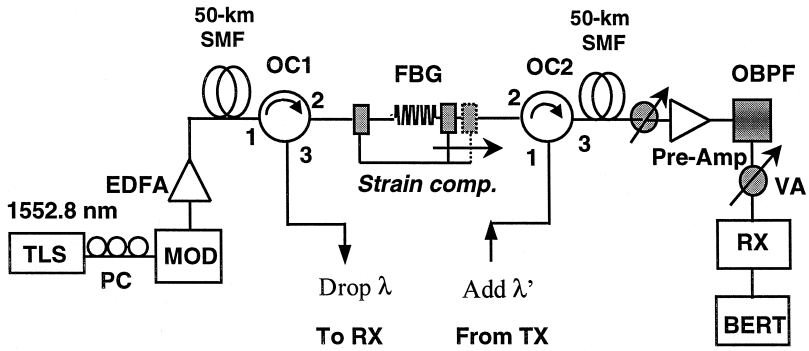

Fig. 3. Experimental setup: TLS: tunable laser source. MOD: modulator. OBPF: optical bandpass filter. RX: optical receiver. BERT: bit-error-rate test set.

about 11.0 dBm are employed to compensate the fiber loss. A PIN FET receiver with a sensitivity of -38.6 dBm at a bit-error-rate (BER) of 10^{-9} is used to measure the system performance. The inter-port isolation is 50 dB and the insertion loss is 0.9 dB for the three-port OC. The FBG has a reflectivity of 99.9% and the -10, -20 and -30 dB bandwidths of the FBG are 0.20, 0.35 and 0.60 nm, respectively. Instead of using a PZT for strain tuning, the FBG is stuck onto two translation stages for feasible study of wavelength pass-through and add/drop. The central reflected wavelength of the FBG is 1552.8 nm without strain and 1554.0 nm when strain is applied ($\Delta\lambda_{\mathrm{STRAIN}} = 1.2$ nm). The strain applied to FBG is about 1000 $\mu\varepsilon$ measured by using a strain gauge for wavelength-shift of 1.2 nm.

4. Results and discussion

The channel assignment for an N-channel WDM system could be based on the International Telecommunication Union (ITU) proposal of 200-GHz (1.6-nm) spacing. Without applying strain, the central reflective wavelength of FBG_i could be assigned such as $\lambda_i = \lambda_1 + (i-1) \times 1.6$ (in nm) for $1 \le i \le N$. FBG_1, $\mathrm{FBG}_2 \ldots \mathrm{FBG}_N$ are located consecutively, from the left-hand side to the right-hand side, as shown in Fig. 2, between the two three-port elements. Homodyne crosstalk may be induced from the add port to the drop port, or the input port to the output port. To suppress the homodyne crosstalk effect, the central reflective wavelength of FBG_i may be shifted between $\lambda_i + \Delta\lambda_{30\mathrm{dB}}$ and $\lambda_{i+1} - \Delta\lambda_{30\mathrm{dB}}$ when strain is applied, where $\Delta\lambda_{30\mathrm{dB}}$ is the -30 dB stopband bandwidth of the FBG with a value of about 0.6 nm in this experiment. Thus, the appropriately tuning range for FBG is from 0.6 to 1.0 nm. For example, if the central wavelength of FBG_i is shifted from λ_i to $\lambda_{i+1} - \Delta\lambda_{30\mathrm{dB}}$ and λ_{i+1} is dropped by the FBG_{i+1} at the same time, -30 dB homodyne crosstalk may contaminate the dropped channel of λ_{i+1}. Nevertheless, the -30 dB crosstalk induce power penalty is nearly 0 dB by experimental measurement and only 0.3 dB even using the worst case Gaussian approximation [16]. Based on previous analysis, the acceptable tuning range is 1.6 nm $- 2 \times \Delta\lambda_{30\mathrm{dB}}$ in this example. One extra high reflectivity of FBG (over 99.9%) was used during our measurement. Also, the homodyne crosstalk effect due to the 0.1% (-30 dB) transmission of optical power is negligible. Also, each laser wavelength and its corresponding FBG were carefully adjusted to avoid wavelength misalignment. Fig. 4 shows the measured BER of the WADM against the received power for the baseline signal (0 km), the dropped signal (50 km) and the pass-through signal (100 km). For the measurement of pass-through channel, the data was measured by tuning the central wavelength of FBG of 1.2 nm away from its initial wavelength. Note that the performance of drop channel is even a little bit better than that of the back to back condition, due to the fact that the majority of amplified stimulated emission (ASE) noise from the EDFA is filtered out when the signal is reflected by the FBG. A negligible power penalty of only 0.2 dB for the passing channel

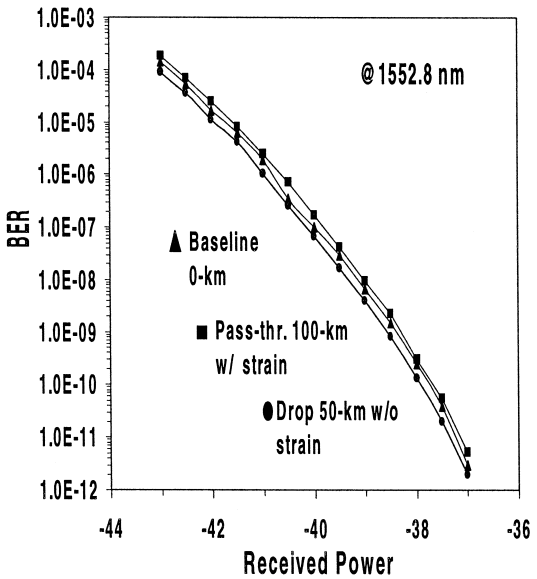

Fig. 4. Measured BER performance of the WADM at 1552.8 nm against the received power for the back-to back (0 km), dropped (50 km) and pass-through (100 km) conditions in a 2.5-Gb/s externally modulated system.

over a 100-km transmission is observed compared to the back-to-back transmission. A similar result could be obtained from the reflection-type OXC device except that the ASEs of EDFAs result from different fiber links will travel along with the signals. However, the ASEs will not degrade the system performance if only the SNR of each channel is above a certain level, say, 15 dB. Hence, the WADM/OXC architecture represents a thoroughly optical transparent ability. Each wavelength path is represented by its corresponding FBG with a roughly rectangular shape and a low sideband loss.

5. Conclusion

A reconfigurable all-fiber WADM and reflection type OXC device based on ST-FBGs integrated three-port elements are proposed. One-channel added/dropped experiment of the WADM device is investigated over a 50-km and a 100-km standard fiber for the dropped channel and the pass-through channel in a 2.5 Gb/s system. Compared to back-to-back transmission, no power penalty is found. The FBG-based WADM as well as the closely related OXC device with the features of dynamically wavelength-selective function, high signal-to-noise contrast ratio, potentially low crosstalk, uniform and low insertion loss, low cost, high scalability and cascadability may provide vast applications in the optical networks.

Acknowledgements

The authors are indebted to P.-Y. Chien and K.-Y. Hsu for equipment support and helpful discussion. The BER measurement of this paper were conducted in the Lightwave Communication Laboratory, Department of Information Engineering, The Chinese University of Hong Kong, Shatin, Hong Kong.

References

[1] C.A. Brackett, J. Lightwave Technol. 14 (1996) 936.
[2] Y.D. Jin, M. Kavehrad, IEEE Photon. Technol. Lett. 7 (1995) 1300.
[3] Multi-wavelength optical technology and networks, J. Lightwave Technol., 14 June, 1996.
[4] R.A. Spanke, IEEE Commun. Mag. 25 (1987) 42.
[5] W.D. Zhong, J.P.R. Lacey, R.S. Tucker, J. Lightwave Technol. 14 (1996) 1613.
[6] Y.-K. Chen, W.I. Way, IEEE Photon. Photon. Lett. 6 (1994) 1122.
[7] K. Okamoto, K. Takiguchi, Y. Ohmori, Electron. Lett. 32 (1996) 1471.
[8] N.A. Riza, Optics in Computing OC'98, vol. 3490, Bruges, Belgium, 1998, p. 335.
[9] H. Okayama, Y. Ozeki, T. Kamijoh, C.Q. Xu, I. Asabayashi, Electron. Lett. 33 (1997) 403.
[10] Y.-K. Chen, C.-C. Lee, J. Lightwave Technol. 16 (1998) 1746.
[11] D.R. Hjelme, H. Storoy, J. Skaar, OFC'98, paper TuJ6, San Jose, CA, USA.
[12] G.A. Ball, W.W. Morey, Opt. Lett. 19 (1994) 1979.
[13] B.J. Eggleton, G. Lenz, N. Litchinitzer, D.B. Patterson, R.E. Slusher, IEEE Photon. Technol. Lett. 9 (1997) 1403.
[14] N.A. Riza, J. Chen, Opt. Lett. 23 (1998) 945.
[15] K.T. Grattan, B.T. Meggitt, Optical Fiber Sensor Technology, 1st ed., Chapman and Hall, 1995 (Section 9.7).
[16] K.-P. Ho, J. Lightwave Technol. 17 (1999) 149.